

Supporting Information for

## Surface Passivation and Energetic Modification Suppress Nonradiative Recombination in Perovskite Solar Cells

Wei Dong<sup>1</sup>, Wencheng Qiao<sup>1</sup>, Shaobing Xiong<sup>2</sup>, Jianming Yang<sup>2</sup>, Xuelu Wang<sup>1</sup>, Liming Ding<sup>3</sup>,  
\*, Yefeng Yao<sup>1, \*</sup>, Qinye Bao<sup>2, 4, \*</sup>

<sup>1</sup>Shanghai Key Laboratory of Magnetic Resonance, East China Normal University, Shanghai 200241, P. R. China

<sup>2</sup>School of Physics and Electronic Science, East China Normal University, Shanghai 200241, P. R. China

<sup>3</sup>Center for Excellence in Nanoscience (CAS), Key Laboratory of Nanosystem and Hierarchical Fabrication (CAS), National Center for Nanoscience and Technology, Beijing 100190, P. R. China

<sup>4</sup> Collaborative Innovation Center of Extreme Optics, Shanxi University, Taiyuan, Shanxi 030006, P. R. China

\* Corresponding authors. E-mail: [ding@nanocr.cn](mailto:ding@nanocr.cn) (Liming Ding), [yfyao@phy.ecnu.edu.cn](mailto:yfyao@phy.ecnu.edu.cn) (Yefeng Yao), [qybao@clpm.ecnu.edu.cn](mailto:qybao@clpm.ecnu.edu.cn) (Qinye Bao)

### Supplementary Figures and Tables

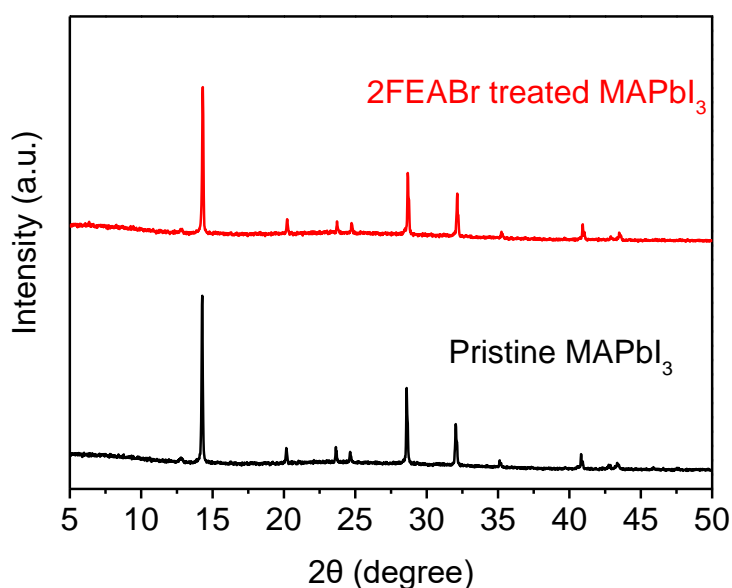


**Fig. S1** XRD patterns of pristine and 2FEABr treated perovskite films

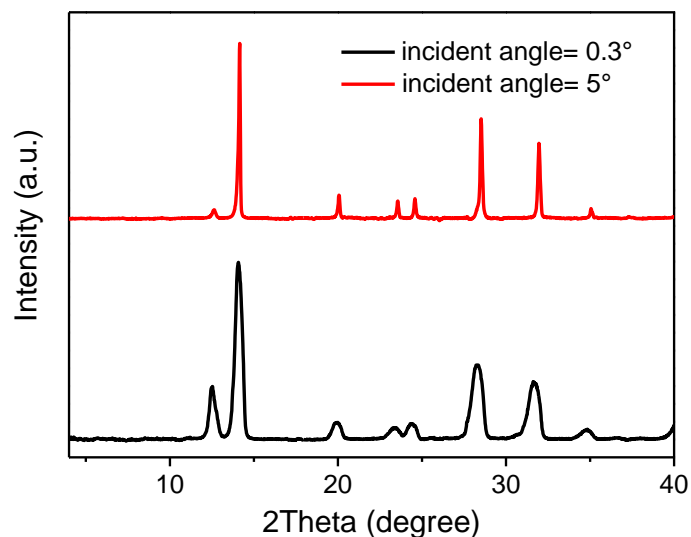


**Fig. S2** GIXRD patterns of 2FEABr treated MAPbI<sub>3</sub> film

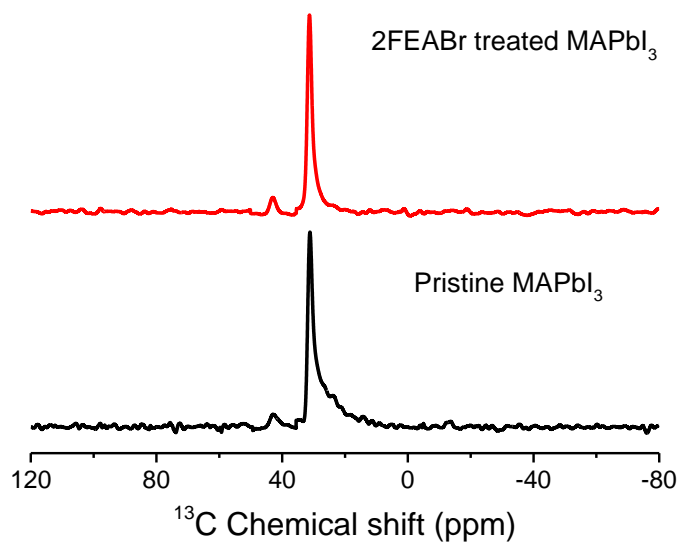


**Fig. S3** <sup>13</sup>C MAS SS-NMR spectra of pristine and 2FEABr treated MAPbI<sub>3</sub>

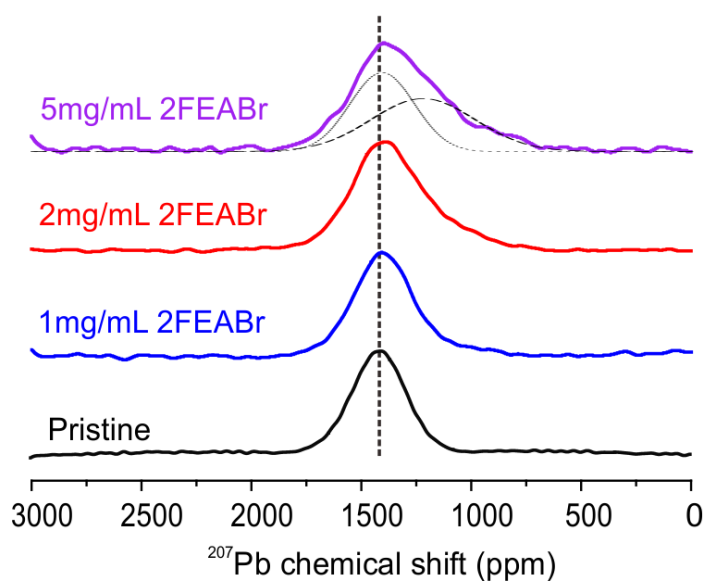


**Fig. S4** <sup>207</sup>Pb NMR spectra of MAPbI<sub>3</sub> treated with different 2FEABr concentrations

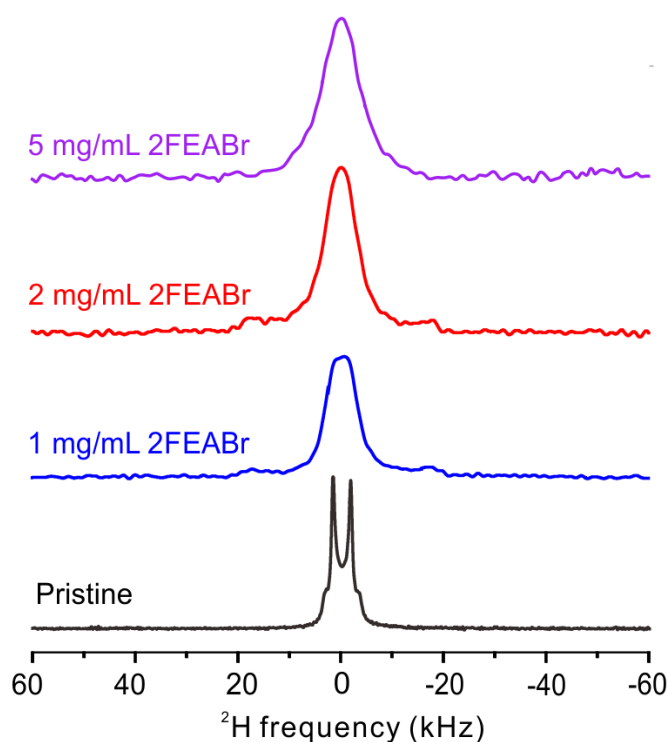


**Fig. S5**  $^2\text{H}$  NMR spectra of  $\text{MAPbI}_3$  treated with different 2FEABr concentrations

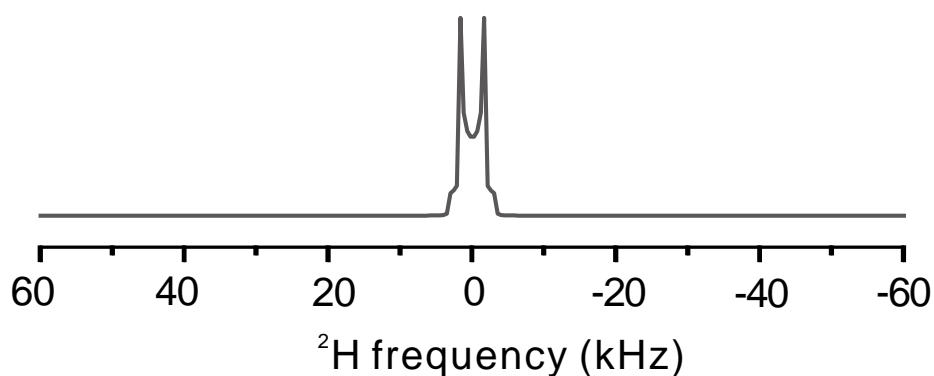


**Fig. S6** The corresponding pattern simulation of Pake line shape in  $^2\text{H}$  NMR spectrum of pristine  $\text{MAPbI}_3$  sample. The inclined angle  $\theta$  is the angle between  $C_n$  axis and  $R_c$  axis in the model in Figure 1g. The  $\theta$  value obtained from the pattern simulation is  $58.9^\circ$

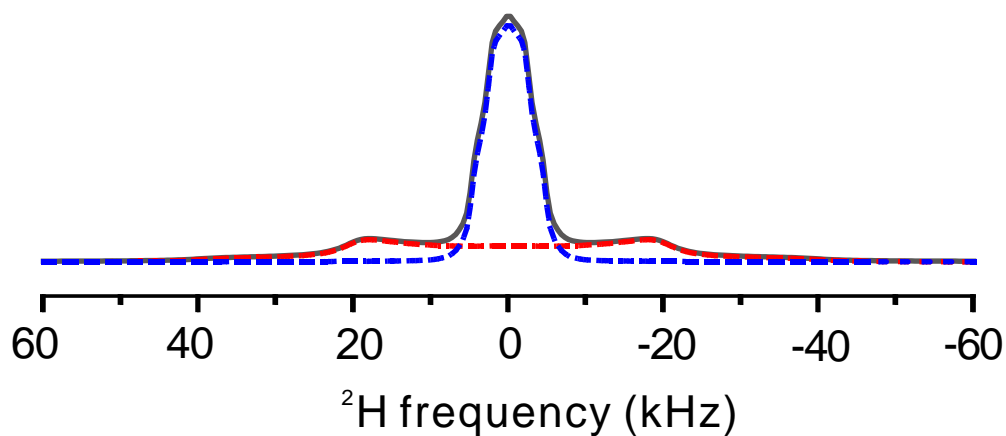


**Fig. S7** The corresponding pattern simulation of the line shape of  $^2\text{H}$  NMR spectrum of 2FEABr treated  $\text{MAPbI}_3$

The interval of  $\theta$  can be estimated from the Gaussian distribution:

$$f(\theta) = \frac{1}{\sigma\sqrt{2\pi}} \exp\left[-\frac{(\theta - \theta_0)^2}{2\sigma^2}\right]$$

Where the  $\theta$  values are assumed to be distributed about a mean value  $\theta_0$  ( $58.9^\circ$ ) according to the Gaussian distribution with standard deviation  $\sigma$ . The obtained  $\sigma$  values from the simulation results are summarized in **Table S1**.

**Table S1**  $\sigma$  values obtained from the simulated  $\theta$  distribution of  $\text{MA}^+$  cations motion model

2FEABr concentrations	pristine	1 mg/mL	2 mg/mL	5 mg/mL
standard deviation $\sigma$ ( $^\circ$ )	0	7	13	20

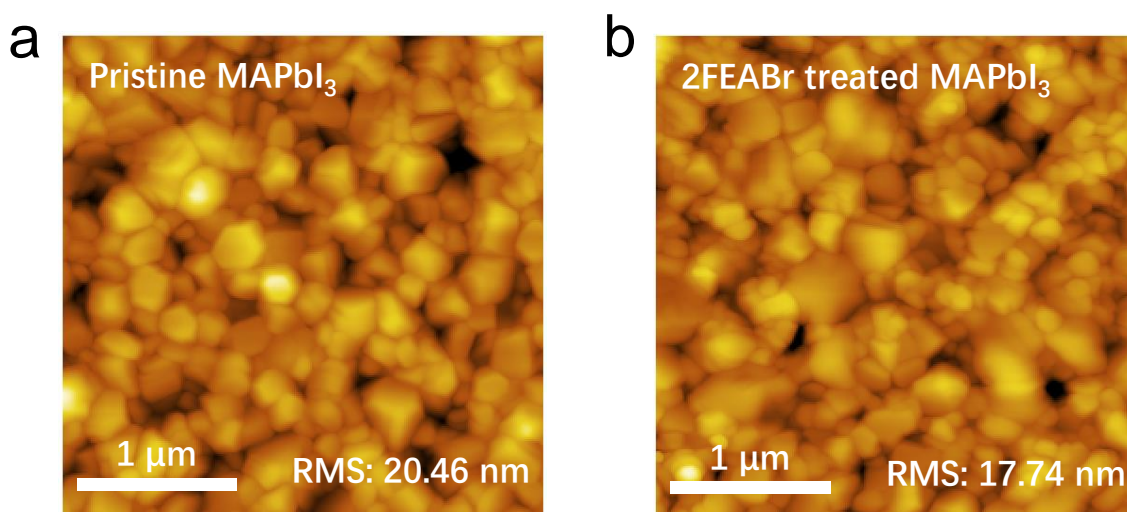


**Fig. S8** AFM images of (a) pristine and (b) 2FEABr treated perovskite films

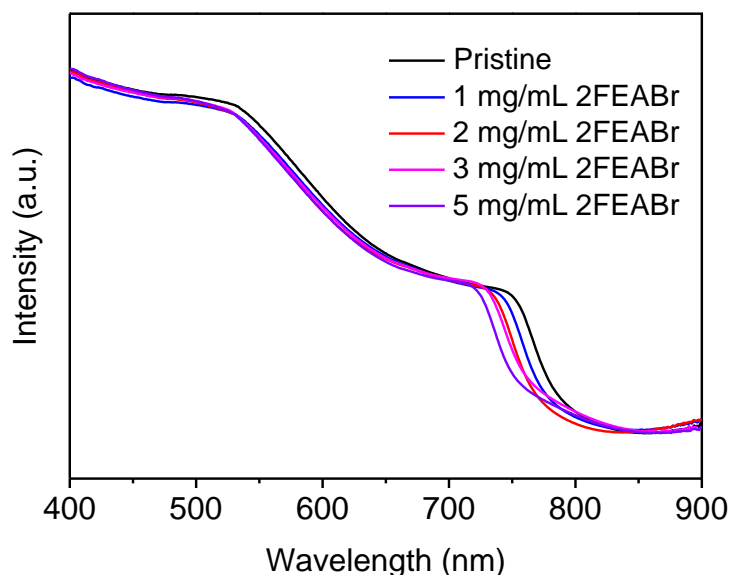


**Fig. S9** UV-vis absorption spectra of  $\text{MAPbI}_3$  films treated with different 2FEABr concentrations

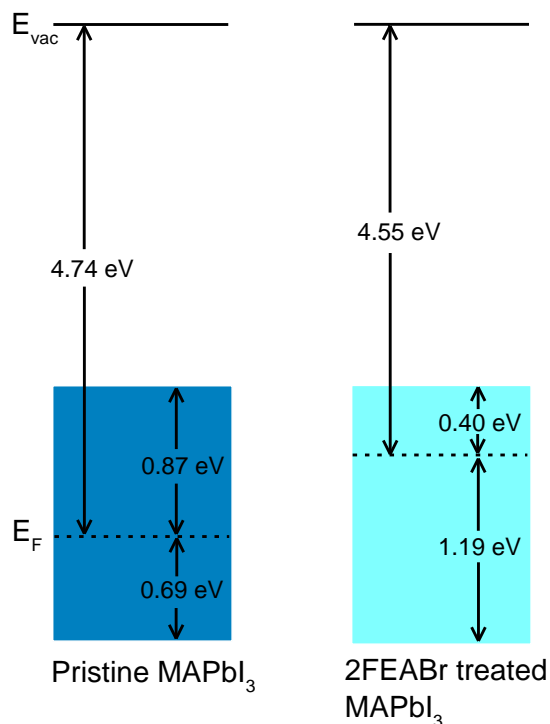


**Fig. S10** Energy level diagram of pristine and 2FEABr treated perovskite film derived from UPS spectra

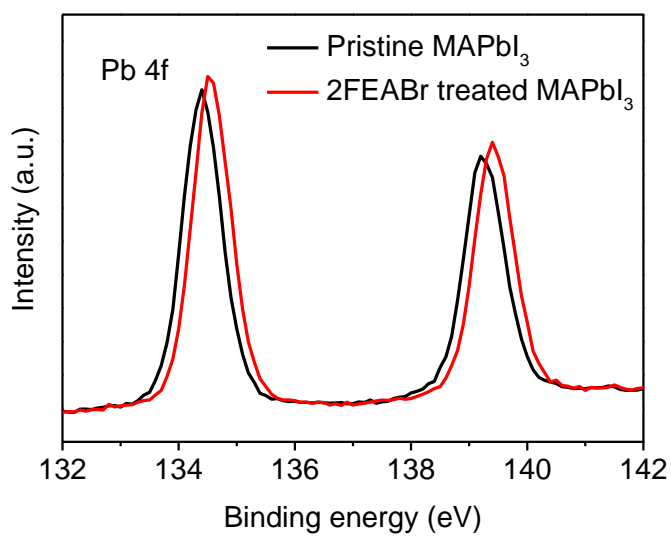


**Fig. S11** Pb 4f XPS spectra of pristine and 2FEABr treated MAPbI<sub>3</sub> film

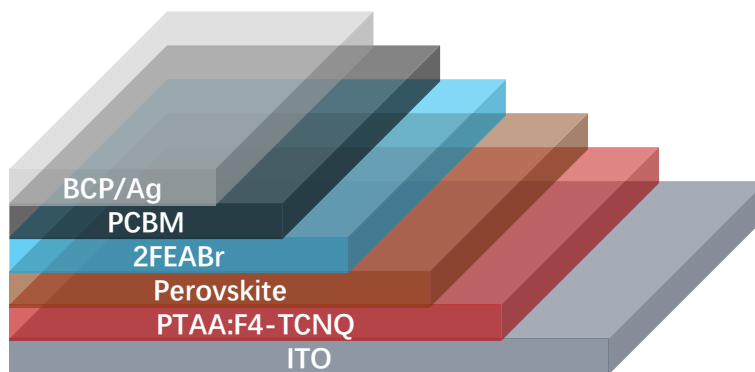


**Fig. S12** Configuration of p-i-n structured PSC in this study

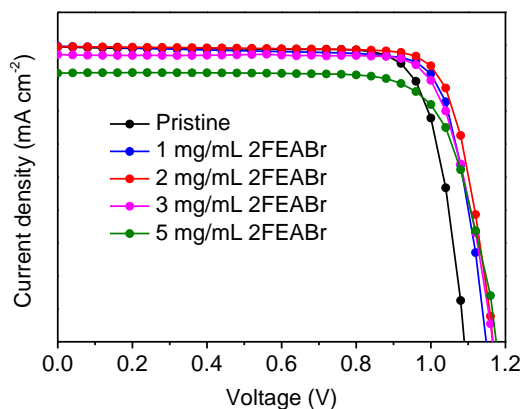


**Fig. S13** J-V characteristic of champion devices treated with different 2FEABr concentrations

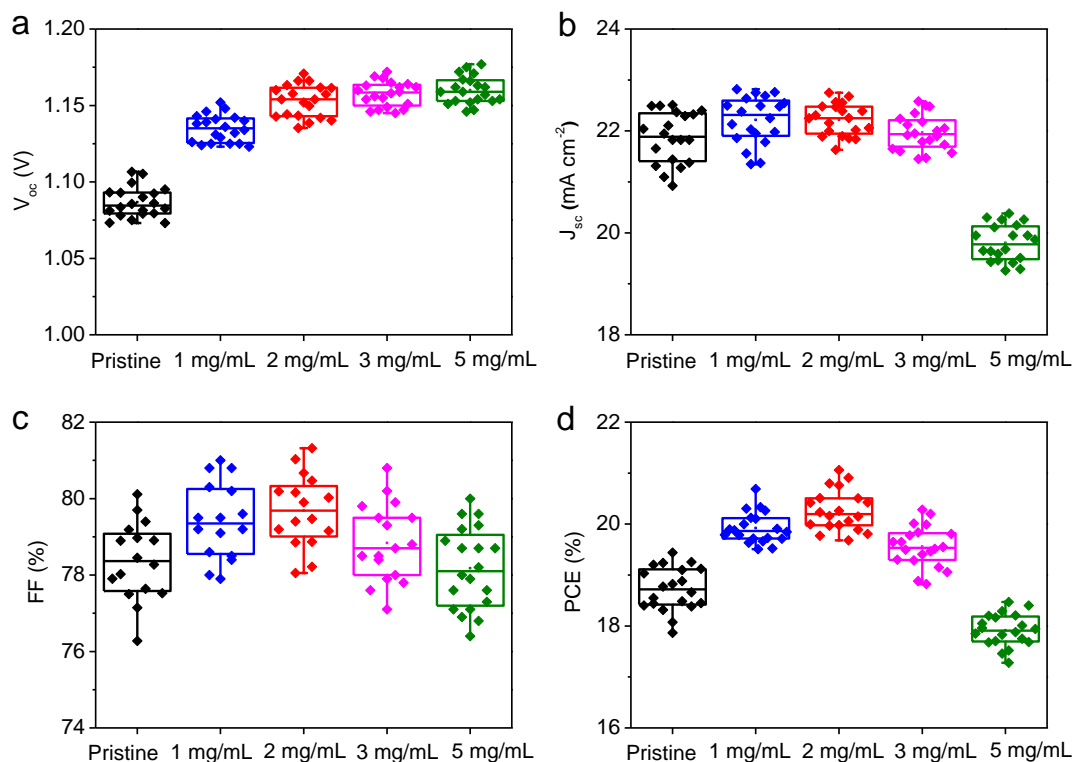


**Fig. S14** Photovoltaic parameter distributions of the devices treated with different concentrations of 2FEABr: (a)  $V_{oc}$ , (b)  $J_{sc}$ , (c) FF, and (d) PCE

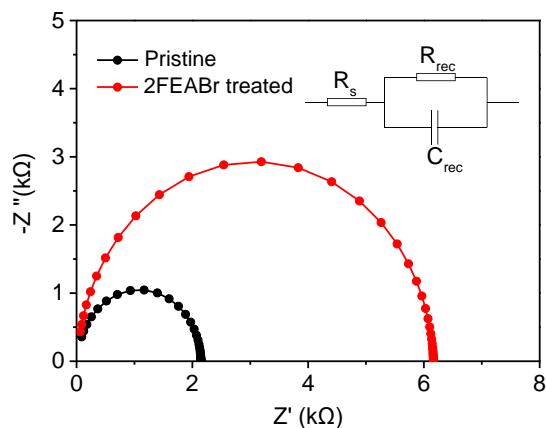


**Fig. S15** Nyquist plots of electrical impedance spectra of the PSCs based on pristine and 2FEABr treated  $\text{MAPbI}_3$

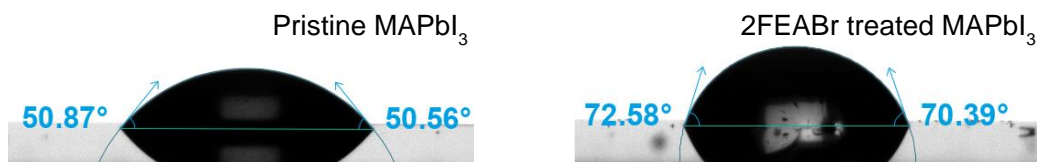


**Fig. S16** Water contact angles of pristine and 2FEABr treated MAPbI<sub>3</sub> film

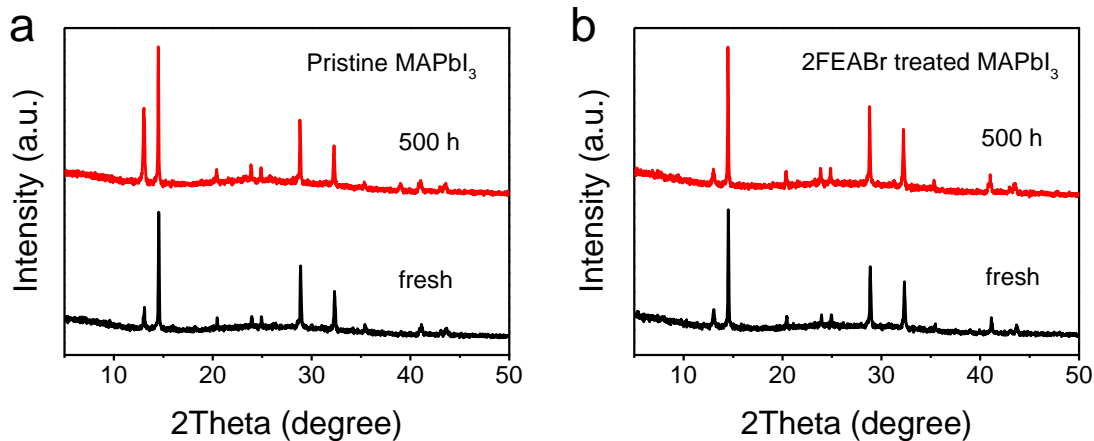


**Fig. S17** The XRD patterns of pristine and 2FEABr treated MAPbI<sub>3</sub> films before and after 500 h calcination at 340 K

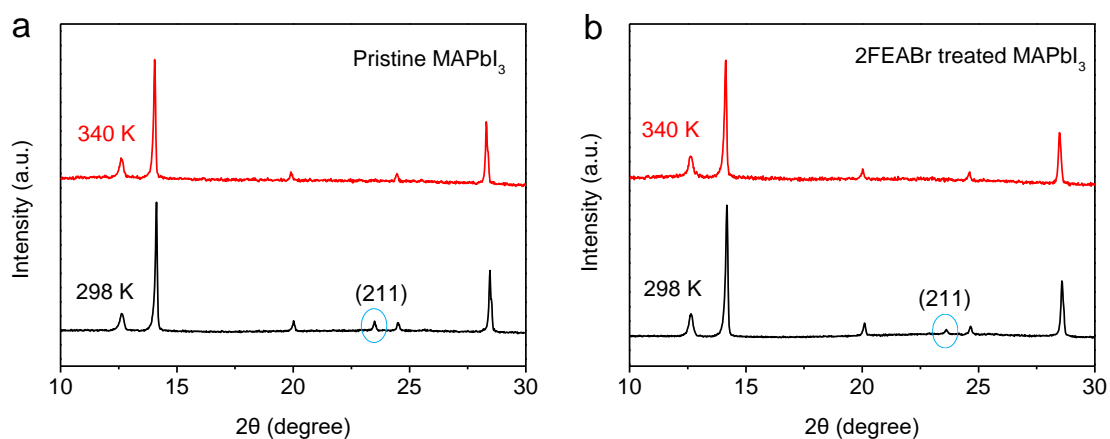


**Fig. S18** XRD patterns of the pristine and 2FEABr treated MAPbI<sub>3</sub> films measured at 298 K and 340 K, respectively. The characterized peak at 23.5° is attributed to the (211) plane of tetragonal phase of MAPbI<sub>3</sub>

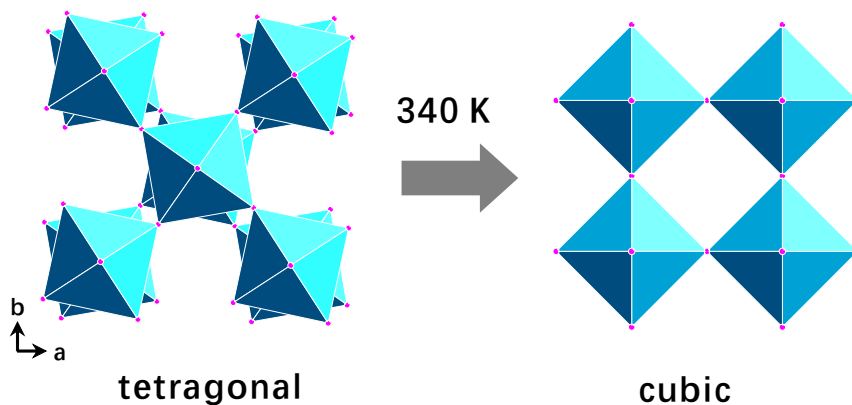


**Fig. S19** Schematic illustration of phase transition for MAPbI<sub>3</sub> perovskite from tetragonal phase to cubic phase

**Table S2** The fitted parameters of the TRPL spectra

	$\tau_1$ (ns)	A1 (%)	$\tau_2$ (ns)	A2 (%)
<b>Pristine</b>	20.5	72.9	101.8	27.1
<b>2FEABr treated</b>	32.3	68.4	145.6	31.6

**Table S3** Photovoltaic parameters of the devices with different 2FEABr concentrations

<b>2FEABr concentration</b>	<b>Voc (V)</b>	<b>Jsc (mA/cm<sup>2</sup>)</b>	<b>FF</b>	<b>PCE (%)</b>
Pristine	1.090	22.38	0.797	19.44
1 mg/mL	1.148	22.49	0.802	20.69
2 mg/mL	1.166	22.39	0.807	21.06
3 mg/mL	1.165	21.79	0.799	20.28
5 mg/mL	1.175	20.38	0.771	18.47

**Table S4** The fitting results of the equivalent circuit of Nyquist plots

<b>PSCs</b>	<b>R<sub>s</sub> (<math>\Omega</math>)</b>	<b>R<sub>rec</sub> (k<math>\Omega</math>)</b>	<b>C<sub>rec</sub> (nF)</b>
<b>Pristine</b>	22	2.13	4.83
<b>2FEABr treated</b>	14	6.15	5.51